Acidic Properties and Catalytic Activity of Titanium Sulfate Supported on TiO_2

Jong Rack Sohn,* Si Hoon Lee,† Park Won Cheon, and Hea Won Kim‡

Department of Applied Chemistry, Engineering College, Kyungpook National University, Daegu 702-701, Korea
†Environment Research Team, Research Institute of Industrial Science and Technology, Kyungbuk, Pohang 790-330, Korea
‡Department of Industrial Chemistry, Kyung Il University, Kyungsan 712-701, Korea
Received November 29, 2003

Titanium sulfate supported on TiO_2 was prepared by impregnation of powdered TiO_2 with an aqueous solution of titanium sulfate followed by calcining in air at high temperature. For $Ti(SO_4)_2/TiO_2$ samples calcined at 300 °C, no diffraction lines of titanium sulfate are observed at $Ti(SO_4)_2$ loading up to 30 wt%, indicating good dispersion of $Ti(SO_4)_2$ on the surface of TiO_2. The acidity of the catalysts increased in proportion to the titanium sulfate content up to 20 wt% of $Ti(SO_4)_2$. 20 wt% $Ti(SO_4)_2/TiO_2$ calcined at 300 °C exhibited maximum catalytic activities for 2-propanol dehydration and cumene dealkylation. The catalytic activities for these reactions, were correlated with the acidity of catalysts measured by ammonia chemisorption method.

Key Words : Titanium sulfate supported on TiO_2, Characterization, 2-Propanol dehydration, Cumene dealkylation, Acidic properties

Intorduction

Acid catalysis[1,2] plays a key role in many important reactions of the chemical and petroleum industries, and environmentally benign chemical processes. Liquid superacids[3] based on HF, which are efficient and selective at room temperature, are not suitable for industrial processes due to separation problems tied with environmental regulations. Conventional industrial acid catalysts, such as sulfuric acid, $AlCl_3$, and BF_3, have unavoidable drawbacks because of their severe corrosivity and high susceptibility to water. Thus the search[2,4,5] for environmentally benign heterogeneous catalysts has driven the worldwide research of new materials as a substitute for current liquid acids and halogen-based solid acids. Among them sulfated oxides, such as sulfated zirconia, titania, and iron oxide exhibiting high thermostability, superacidic property, and high catalytic activity, have evoked increasing interest.[2,4,5] The strong acidity of zircona-supported sulfate has attracted much attention because of its ability to catalyze many reactions such as cracking, alkylation, and isomerization. The potential for a heterogeneous catalyst has yielded many research output on the catalytic activity of sulfated zirconia materials.[4-9]

Sulfated zirconia incorporating Fe and Mn has been shown to be highly active for butane isomerization, catalyzing the reaction even at room temperature.[10,11] Such promotion in activity of catalyst has been confirmed by several other research group.[12-14] Coelho *et al*.[15] have discovered that the addition of Ni to sulfated zirconia results in an activity enhancement comparable to that caused by the addition of Fe and Mn. It has been reported by several workers that the addition of platinum to zirconia modified by sulfate ions enhances catalytic activity in the skeletal isomerization of alkanes without deactivation when the reaction is carried out in the presence of hydrogen.[16-18] The high catalytic activity and small deactivation can be explained by both the elimination of the coke by hydrogenation and hydrogenolysis,[16] and the formation of Brönsted acid sites from H_2 on the catalysts.[17] Recently, Hino and Arata reported zirconia-supported tungsten oxide as an alternative material in reaction requiring strong acid sites.[4,19] Several advantages of tungstate, over sulfate, as dopant include that it does not suffer from dopant loss during thermal treatment and it undergoes significantly less deactivation during catalytic reaction.[20]

Many metal sulfates generate fairly large amounts of acid sites of moderate or strong strength on their surfaces when they are calcined at 400-700 °C.[2,21] The acidic property of metal sulfate often gives high selectivity for diversified reaction such as hydration, polymerization, alkylation, cracking, and isomerization.[2,20] Structural and physicochemical properties of supported metal sulfates are considered to be in different states compared with bulk metal sulfates because of their interaction with supports.[22-24] It came to our attention that titanium sulfate catalysts supported on TiO_2 have not been reported up to now.

In this investigation, titanium oxide was prepared by a precipitation method and was used as a support. This paper describes acidic properties of titanium sulfate supported on TiO_2 and its activity in acid catalysis. The characterization of the samples was performed by means of Fourier transform infrared (FTIR) spectroscopy, X-ray diffraction (XRD), differential scanning calorimetry (DSC), and surface area measurements. For the acid catalysis, 2-propanol dehydration and cumene dealkylation were used as test reactions.

Experimental Section

Catalyst preparation. The precipitate of $Ti(OH)_4$ was obtained by adding aqueous ammonia slowly into a mixed aqueous solution of titanium tetrachloride and hydrochloric acid at 60 °C with stirring until the pH of the mother liquor

*To whom correspondence should be addressed. Tel: +82-53-950-5585; Fax: +82-53-950-6594; e-mail: jrsohn@knu.ac.kr

reached about 8.[25] The precipitate thus obtained was washed thoroughly with distilled water until chloride ion was not detected, and was dried at room temperature for 12 h. The dried precipitate was powdered below 100 mesh. Catalysts containing various titanium sulfate contents were prepared by the impregnation of $Ti(OH)_4$ powder with an aqueous solution of $Ti(SO_4)_2 \cdot 4H_2O$ followed by calcining at different temperatures for 2 h in air. This series of catalysts is denoted by the weight percentage of titanium sulfate. For example, 20-$Ti(SO_4)_2/TiO_2$ indicates the catalyst containing 20 wt% of $Ti(SO_4)_2$.

Characterization and catalytic study. FTIR spectra were obtained in a heatable gas cell at room temperature using Mattson Model GL6030E spectrophotometer. The wafers contained about 9 mg/cm^2 self-supporting catalyst. Prior to obtaining the spectra the samples were heated under vacuum at 25-400 °C for 1 h. Catalysts were checked in order to determine the structure of the prepared catalysts by means of a Philips X'pert-APD X-ray diffractometer, employing Ni-filtered Cu K_α radiation. DSC measurements were performed by a PL-STA model 1500H apparatus in air, and the heating rate was 5 °C per minute. For each experiment 10-15 mg of sample was used.

The acid strength of catalyst was measured qualitatively using a series of the Hammett indicators.[26] The catalyst in a glass tube was pretreated at 500 °C for 1 h and filled with dry nitrogen. For the determination of acid strength of the catalyst the color changes of indicators were observed by spot test. Chemisorption of ammonia was employed as a measure of acidity of catalysts. The amount chemisorbed was obtained as the irreversible adsorption of ammonia.[24] Thus the first adsorption of ammonia at 20 °C and 300 Torr was followed by evacuation at 230 °C for 1 h and readsorption at 20 °C, the difference between two adsorptions at 20 °C giving the amount of chemisorption. The specific surface area was determined by applying the BET method to the adsorption of nitrogen at -196 °C.

2-propanol dehydration was carried at 160 and 180 °C in a pulse micro-reactor connected to a gas chromatograph. Fresh catalyst in the reactor made of 1/4 inch stainless steel was pretreated at 400 °C for 1 h in the nitrogen atmosphere. Diethyleneglycol succinate on Simalite was used as packing material of gas chromatograph and the column temperature was 180 °C for analyzing the product. Catalytic activity for 2-propanol dehydration was represented as mole of propylene converted from 2-propanal per gram of catalyst. Cumene dealkylation was carried out at 250-300 °C in the same reactor as above. Packing material for the gas chromatograph was Benton 34 on chromosorb W and column temperature was 130 °C. Catalytic activity for cumene dealkylation was represented as mole of benzene converted from cumene per gram of catalyst. Conversions for both reactions were taken as the average of the first to sixth pulse values.

Results and Discussion

Infrared spectra. The IR spectra of 20-$Ti(SO_4)_2/TiO_2$ (KBr disc) calcined at different temperatures (200-800 °C) are given in Figure 1. 20-$Ti(SO_4)_2/TiO_2$ calcined up to 600 °C showed IR absorption bands at 1223, 1139, 1044 and 980 cm^{-1} which are assigned to bidentate sulfate ion[27] coordinated to the metal such as Ti^{4+}. The band at 1625 cm^{-1} is assigned to the deformation vibration mode of the adsorbed water. For 20-$Ti(SO_4)_2/TiO_2$ calcined at 600 °C, the band intensities of sulfate ion decreased considerably because of the partial decomposition of sulfate ion. However, for the sample calcined at 700-800 °C IR bands by the sulfate ion disappeared completely due to the decomposition of sulfate ion.

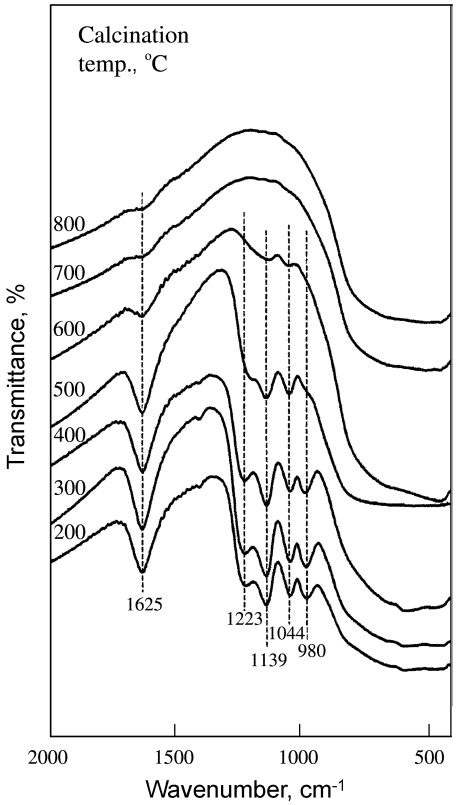

Figure 1. Infrared spectra of 20-$Ti(SO_4)_2/TiO_2$ calcined at different temperatures for 2 h.

In general, for the metal oxides modified with sulfate ion followed by evacuation above 400 °C, a strong band[28-30] assigned to S=O stretching frequency is observed at 1390-1370 cm^{-1}. In this work, the corresponding band for samples exposed to air was not found because water molecules in air were adsorbed on the surfaces of catalysts. These results are very similar to those reported by other authors.[28-30] In a separate experiment IR spectra of self-supported 20-$Ti(SO_4)_2/TiO_2$ after evacuation at 25-500 °C for 2 h were examined. As shown in Figure 2, an intense band at 1370-1382 cm^{-1} accompanied by broad and intense bands below 1250 cm^{-1} was observed due to the overlapping of the TiO_2 skeletal vibration, indicating the presence of different adsorbed species depending on the treatment conditions of the sulfated sample.[29] At 100 °C an asymmetric stretching band of S=O bonds was not observed because water molecules are adsorbed on the surface of 20-$Ti(SO_4)_2/TiO_2$.[30-32] At 200 °C

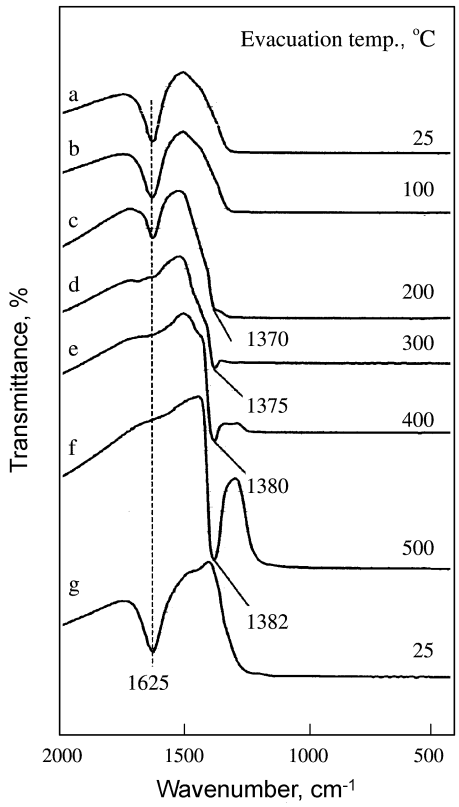

Figure 2. Infrared spectra of 20-$Ti(SO_4)_2/TiO_2$ evacuated at different temperatures.

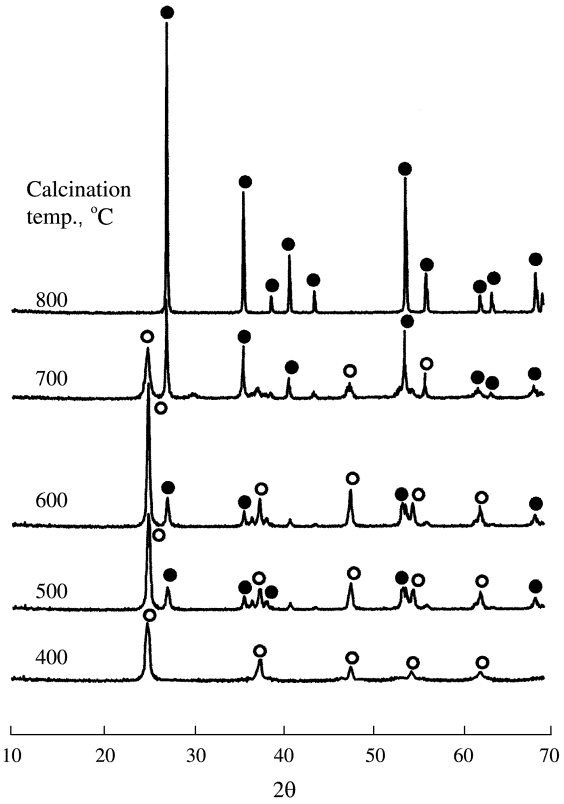

Figure 3. X-ray diffraction patterns of TiO_2 calcined at different temperatures for 2 h: ○, anatase phase of TiO_2; ●, rutile phase of TiO_2.

the S=O stretching band appeared as a shoulder at 1370 cm^{-1}. The band at 1625 cm^{-1} in Figure 2 is assigned to the deformation vibration mode of the adsorbed water and the band intensity decreases with the evacuation temperature. The band intensity increased with the evacuation temperature and the position of band shifted to a higher wavenumber. That is, the higher the evacuation temperature, the larger was the shift of the asymmetric stretching frequency of the S=O bonds. It is likely that the surface sulfur complexes formed by the interaction of oxides with sulfate ions in highly active catalysts have a strong tendency to reduce their bond order by the adsorption of basic molecules such as H_2O.[30-32] When the 20-$Ti(SO_4)_2/TiO_2$ sample evacuated at 500 °C was exposed to air at 25 °C, the drastic shift of the IR band from 1382 cm^{-1} to lower wavenumber (not shown due to the overlaps with skeletal vibration band of TiO_2) occurred because of the adsorption of water, resulting in the appearance of adsorbed water band at 1625 cm^{-1} [(see Figure 2(g))]. Consequently, as shown in Figure 2, an asymmetric stretching band of S=O bonds for the sample evacuated at a lower temperature appears at a lower frequency compared with that for the sample evacuated at higher temperature because the adsorbed water reduces the bond order of S=O from a highly covalent double-bond character to a lesser double-bond character.

Crystalline structure of $Ti(SO_4)_2/TiO_2$. The crystalline structure of catalysts calcined in air at different temperatures for 2 h were checked by X-ray diffraction. In the case of pure TiO_2, most of TiO_2 calcined at 400 °C was present as anatase form to X-ray diffraction. However, as shown in Figure 3, the amount of anatase increased with increasing the calcination temperature up to 600 °C, indicating that amorphous TiO_2 was transformed into anatase form. From 500 °C, a tiny amount of anatase TiO_2 was transformed into rutile form and the amount increased with the calcination temperature, showing the complete transformation from anatase form to rutile at 800 °C. A two phase mixture of the anatase and rutile was observed at 500-700 °C.

For the 20-$Ti(SO_4)_2/TiO_2$ calcined at 300-800 °C, X-ray diffraction data, as shown in Figure 4, indicated only an anatase phase of TiO_2 at 300-500 °C. The amount of anatase phase increased with the calcination temperature. However, at 600 °C a rutile phase of TiO_2 was observed due to the phase transition from anatase form to rutile. The amount of rutile phase also increased with the calcination temperature, showing only rutile phase at 800 °C due to the complete phase transition from anatase form to rutile. No crystalline phase of $Ti(SO_4)_2$ was observed at any calcination temperature, indicating good dispersion of $Ti(SO_4)_2$ on the surface of TiO_2 due to the interaction between $Ti(SO_4)_2$ and TiO_2. Comparing Figure 3 with Figure 4, it is clear that the phase transition of TiO_2 in $Ti(SO_4)_2/TiO_2$ sample from anatase form to rutile is considerably delayed in comparison with the pure TiO_2 because of the interaction between $Ti(SO_4)_2$ and TiO_2. In view of the X-ray diffraction patterns, the calcination temperatures at which the rutile phase is observed initially

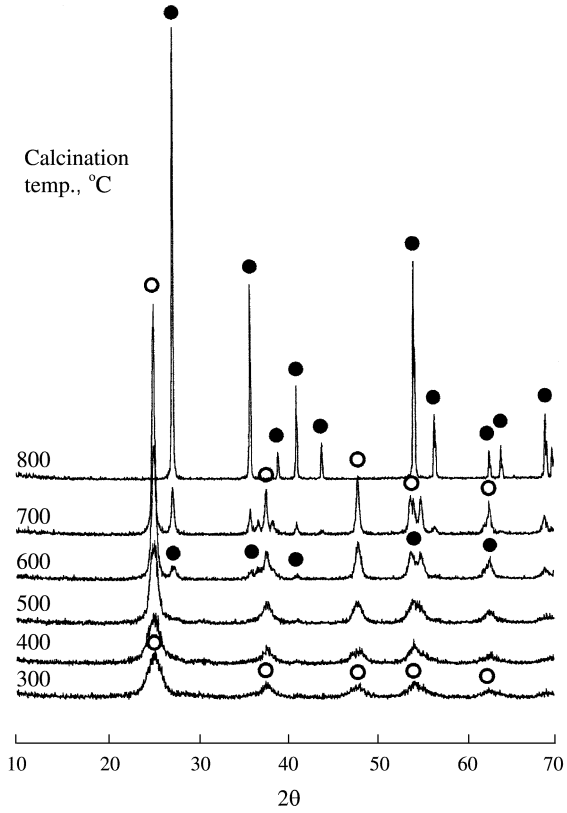

Figure 4. X-ray diffraction patterns of 20-$Ti(SO_4)_2/TiO_2$ calcined at different temperatures for 2 h: ○ , anatase phase of TiO_2; ● , rutile phase of TiO_2.

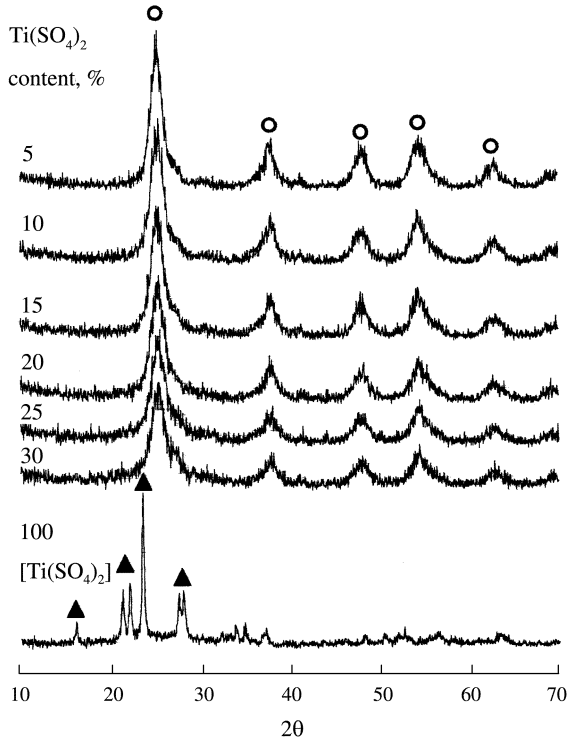

Figure 5. X-ray diffraction patterns of $Ti(SO_4)_2/TiO_2$ having various $Ti(SO_4)_2$ contents and calcined at 300 °C for 2 h: ○ , anatase phase of TiO_2; ▲ , $Ti(SO_4)_2$ phase.

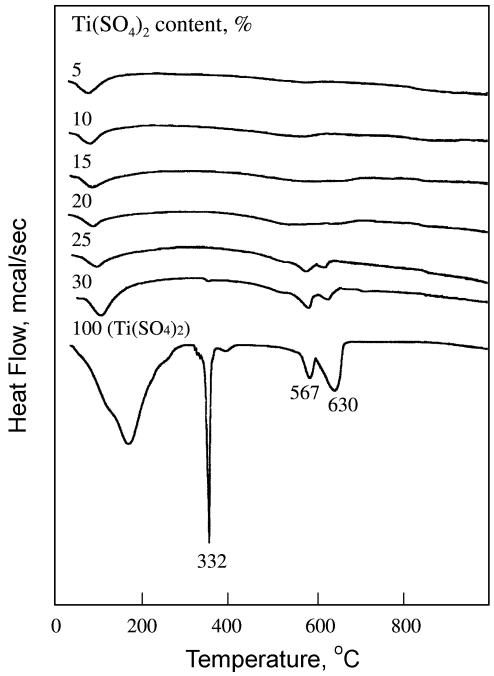

Figure 6. DSC curves of precursors for $Ti(SO_4)_2/TiO_2$ having different $Ti(SO_4)_2$ contents.

are 500 °C for pure TiO_2 and 600 °C for 20-$Ti(SO_4)_2/TiO_2$, respectively. That is, the phase transition temperature for 20-$Ti(SO_4)_2/TiO_2$ is higher by 100 °C than that for pure TiO_2.

The XRD patterns of $Ti(SO_4)_2/TiO_2$ containing different titanium sulfate contents and calcined at 300 °C for 2 h are shown in Figure 5. No diffraction lines of titanium sulfate are observed at low $Ti(SO_4)_2$ loading up to 30 wt%, indicating good dispersion of $Ti(SO_4)_2$ on the surface of TiO_2. For all $Ti(SO_4)_2/TiO_2$ samples, only anatase phase TiO_2 was observed at their calcination temperature 300 °C, indicating that the phase transition of TiO_2 from anatase form to rutile is difficult due to the interaction between $Ti(SO_4)_2$ and TiO_2. However, as shown in Figure 6, the higher is the content of $Ti(SO_4)_2$, the lower is the amount of anatase phase for TiO_2, because the interaction between them prevents the phase transition from amorphous phase to anatase.[25]

Thermal analysis. To examine the thermal properties of precursors of $Ti(SO_4)_2/TiO_2$ samples more clearly, thermal analysis has been carried out and the results are illustrated in Figure 6. For pure $Ti(SO_4)_2 \cdot 4H_2O$ occurs in four steps. The endothermic two peaks around 567 and 630 °C are due to the evolution of SO_3 decomposed from titanium sulfate.[33] Titanium sulfate begins to decompose around 550 °C and the decomposition occurs by two steps, as shown in Figure 6.

However, for $Ti(SO_4)_2/TiO_2$ samples, the DSC patterns are somewhat different from that of $Ti(SO_4)_2 \cdot 4H_2O$. For $Ti(SO_4)_2/TiO_2$ samples, the DSC curve showed endothermic peaks below 200 °C due to the elimination of adsorbed water and hydrated water, and the endothermic peaks around 567 and 630 °C due to the evolution of SO_3 decomposed from the sulfate ion bonded to the surface of TiO_2.[33] Namely, the

Table 1. Specific surface area and acidity of $Ti(SO_4)_2/TiO_2$ calcined at 300 °C for 2 h

Catalyst	Specific surface area (m^2/g)	Acidity (μmol/g)
TiO_2	138	321
5-$Ti(SO_4)_2/TiO_2$	226	436
10-$Ti(SO_4)_2/TiO_2$	260	477
15-$Ti(SO_4)_2/TiO_2$	248	511
20-$Ti(SO_4)_2/TiO_2$	193	557
25-$Ti(SO_4)_2/TiO_2$	88	518
30-$Ti(SO_4)_2/TiO_2$	21	295

Table 2. Specific surface area and acidity of 20-$Ti(SO_4)_2/TiO_2$ calcined at different temperatures for 2 h

Cacination temperature (°C)	Specific surface area (m^2/g)	Acidity (μmol/g)
200	187	540
300	193	557
400	187	385
500	163	274
600	104	167
700	33	53
800	17	20

thermal stability of the sulfate ion bonded to the surface of TiO_2 is the same as that of titanium sulfate. The thermal stability of the sulfate ion bonded to the surface of metal oxide support is different depending on the kind of metal oxide. In the case of $NiSO_4/\gamma$-Al_2O_3 samples reported previously, two endothermic peaks are observed around 785 and 829 °C due to the evolution of SO_3, showing that sulfated species with different thermal stability are present in the samples.[32]

Surface properties. The specific surface areas of samples calcined at 300 °C for 2 h are listed in Table 1. The presence of titanium sulfate influences the surface area in comparison with the pure TiO_2. Specific surface areas of $Ti(SO_4)_2/TiO_2$ samples are larger than that of pure TiO_2 calcined at the same temperature, showing that surface area increases gradually with increasing titanium sulfate loading up to 10 wt%. It seems likely that the interaction between titanium sulfate and TiO_2 prevents catalysts from crystallizing.[22,25] The decrease of surface area for $Ti(SO_4)_2/TiO_2$ samples containing $Ti(SO_4)_2$ above 10 wt% is due to the block of TiO_2 pore by the increased $Ti(SO_4)_2$ loading. The acidity of catalysts calcined at 300 °C, as determined by the amount of NH_3 irreversibly adsorbed at 230 °C,[23,34] is listed in Table 1. The acidity increases with increasing titanium sulfate content up to 20 wt% of $Ti(SO_4)_2$. The acidity is correlated with the catalytic activity for acid catalysis discussed below.

The specific surface area of 20-$Ti(SO_4)_2/TiO_2$ calcined at different temperature are also listed in Table 2. Both values exhibited maxima for the sample calcined at 300 °C. In general, the crystallinity influences on the surface area and acidity of catalyst.[35] As shown in Figure 4, the amount of crystalline material increases with increasing the calcination temperature. Therefore, the decreases for both surface area and acidity of 20-$Ti(SO_4)_2/TiO_2$ above 300 °C are due to the increasing amount of crystalline material at high temperature.

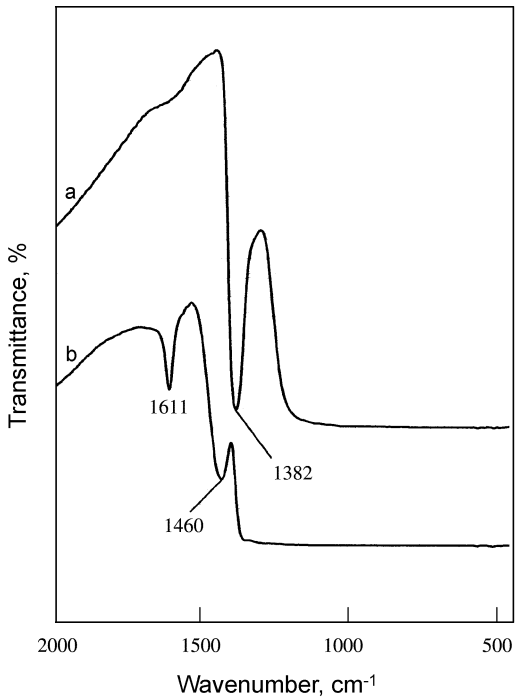

Figure 7. Infrared spectra of NH_3 adsorbed on 20-$Ti(SO_4)_2/TiO_2$: (a) background of 20-$Ti(SO_4)_2/TiO_2$ evacuated at 500 °C for 1 h; (b) ammonia (20 Torr) adsorbed on (a); gas phase evacuated at 230 °C for 1 h.

Infrared spectroscopic studies of ammonia adsorbed on solid surfaces have made it possible to distinguish between Brönsted and Lewis acid sites.[22,32,36] Figure 7 shows the IR spectra of ammonia adsorbed on 20-$Ti(SO_4)_2/TiO_2$ samples evacuated at 500 °C for 1 h. For 20-$Ti(SO_4)_2/TiO_2$ the band at 1460 cm^{-1} is the characteristic peak of ammonium ion, which is formed on the Brönsted acid sites and the absorption peak at 1611 cm^{-1} is contributed by ammonia coordinately bonded to Lewis acid sites,[22,32,36] indicating the presence of both Brönsted and Lewis acid sites on the surface of 20-$Ti(SO_4)_2/TiO_2$ sample. Other samples having different titanium sulfate content also showed the presence of both Lewis and Brönsted acids. The intense band at 1382 cm^{-1} after evacuation at 500 °C is assigned to the asymmetric stretching vibration of S=O bonds having a high double bond nature.[30,37] However, the drastic shift of the IR band from 1382 cm^{-1} to lower wavenumber (not shown due to the overlaps with skeletal vibration bands of TiO_2) after ammonia adsorption [Figure 7(B)] indicates a strong interaction between an adsorbed ammonia molecule and the surface complex. Namely, the surface sulfur compound in the highly acidic catalysts has a strong tendency to reduce the bond order of SO from a highly covalent double-bond character to a lesser double-bond character when a basic ammonia molecule is adsorbed on the catalysts.[30-32]

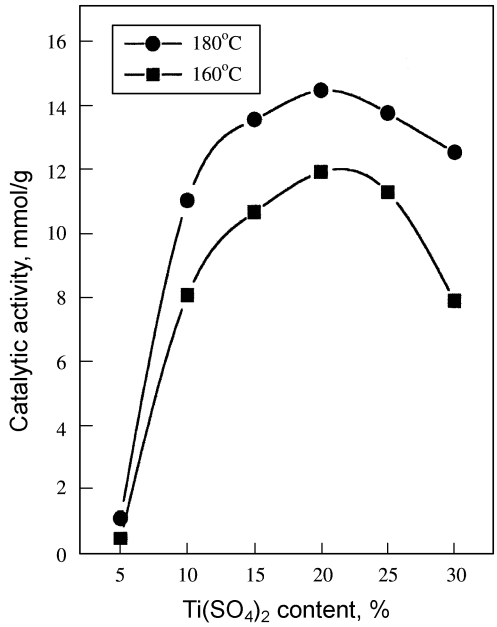

Figure 8. Catalytic activities of $Ti(SO_4)_2/TiO_2$ for 2-propanol dehydration as a function of $Ti(SO_4)_2$ content.

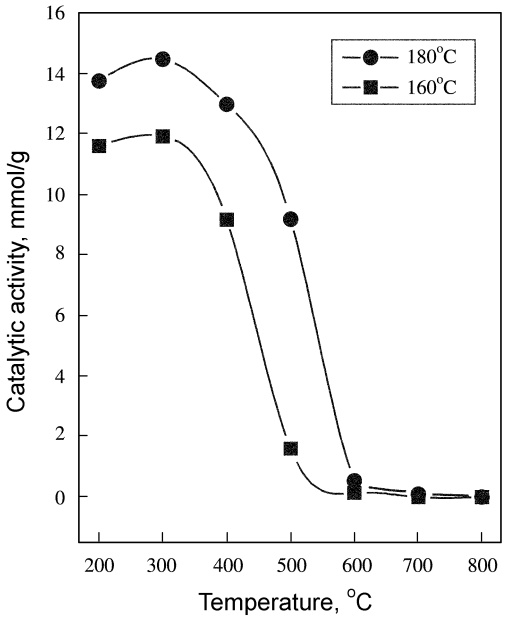

Figure 10. Catalytic activities of 20-$Ti(SO_4)_2/TiO_2$ for 2-propanol dehydration as a function of calcination temperature.

Acid stronger than $H_0 \leq -11.93$, which corresponds to the acid strength of 100% H_2SO_4, are superacids.[1,2,4,38] The strong ability of the sulfur complex to accommodate electrons from a basic molecule such as ammonia is a driving force to generate superacidic properties.[30,37] The 1390-1370 bands representing the asymmetric stretching of S=O is often regarded as the characteristic band of sulfated superacids.[31,39] As shown in Figure 2, the asymmetric stretching bands of S=O after evacuation at 100-500 °C appeared at 1370-1382 cm^{-1} differently depending on the evacuation temperature. The acid strength of $Ti(SO_4)_2/TiO_2$ samples after evacuation at 400 °C for 1 h was also examined by a color change method, using Hammet indicator[40,41] in sulfuryl chloride. The samples were estimated to have $H_0 \leq -14.5$, indicating the formation of superacidic sites. Consequently, $Ti(SO_4)_2/TiO_2$ catalysts would be solid superacids, in analogy with the case of TiO_2 modified with sulfate group.[27]

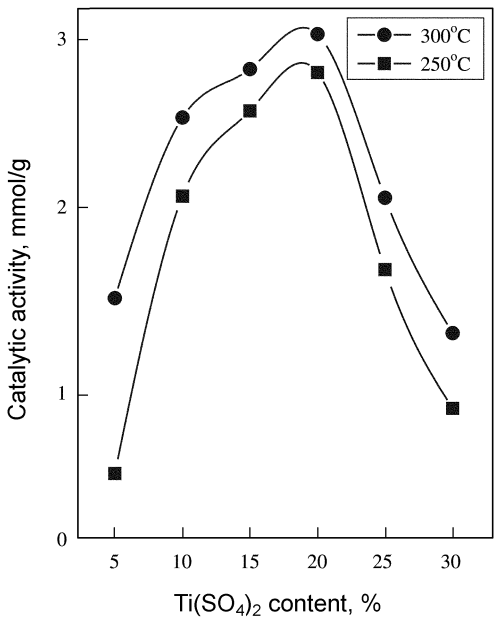

Figure 9. Catalytic activities of $Ti(SO_4)_2/TiO_2$ for cumene dealkylation as a function of $Ti(SO_4)_2$ content.

Catalytic activities for acid catalysis. The catalytic activities for the 2-propanol dehydration are measured and the results are illustrated as a function of $Ti(SO_4)_2$ content in Figure 8, where reaction temperatures are 160-180 °C. In view of Table 1 and Figure 8, the variations in catalytic activity for 2-propanol dehydration are well correlated with the changes of their acidity, showing the highest activity and acidity for 20-$Ti(SO_4)_2/TiO_2$. It has been known that 2-propanol dehydration takes place very readily on weak acid sites.[43,44] Good correlations have been found in many cases between the acidity and the catalytic activities of solid acids. For example the rates of both the catalytic decomposition of cumene and the polymerization of propylene over SiO_2-Al_2O_3 catalysts were found to increase with increasing acid amounts at strength $H_0 \leq +3.3$.[35] It was also reported that the catalytic activity of nickel silicates in the ethylene dimerization as well as in the butene isomerization was closely correlated with the acidity of the catalyst.[45,46]

Cumene dealkylation takes place on relatively strong acid sites of the catalysts.[43,44] Catalytic activities for cumene dealkylation against $Ti(SO_4)_2$ content are presented in Figure 9, where reaction temperature is 250-300 °C. Examining Table 1 and Figure 9, the catalytic activities are also correlated with the acidity. The correlation between catalytic activity and acidity holds for both reactions, cumene dealkylation and 2-propanol dehydration, although the acid strength required to catalyze acid reaction is different depending on the type of reactions. As seen in Figures 8 and

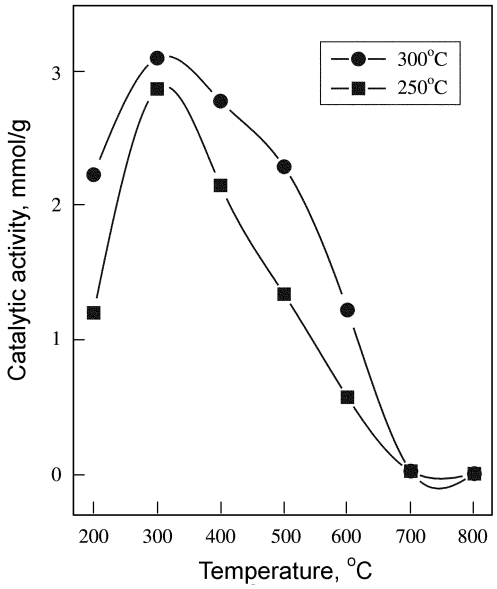

Figure 11. Catalytic activities of 20-$Ti(SO_4)_2/TiO_2$ for cumene dealkylation as a function of calcination temperature.

9, the catalytic activity for cumene dealkylation, in spite of higher reaction temperature, is lower than that for 2-propanol dehydration.

Catalytic activities of 20-$Ti(SO_4)_2/TiO_2$ for 2-propanol dehydration are plotted as a function of calcination temperature in Figure 10. The activities increased with the calcination temperature, giving a maximum at 300 °C and then the activities decreased. Catalytic activities of 20-$Ti(SO_4)_2/TiO_2$ for cumene dealkylation are also plotted as a function of calcination temperature in Figure 11. The activities also exhibited a maximum at 300 °C. The deceased of activity for both reaction above 300 °C can be probably attributed to the fact that the surface area and acidity above 300 °C decrease with the calcination temperature. Considering the experimental results of Table 2, and Figures 10 and 11, it is clear that the catalytic activities for both reactions are correlated with the acidity of catalysts.

Conclusions

This paper has demonotrated that a combination of FTIR, DSC, and XRD can be used to conduct the characterization of $Ti(SO_4)_2/TiO_2$ prepared by impregnation of powdered $Ti(OH)_4$ with titanium sulfate aqueous solution followed by calcining in air. The acidity of catalysts increase in proportion to the titanium sulfate content up to 20 wt% of $Ti(SO_4)_2$. The acid strength of $Ti(SO_4)_2/TiO_2$ samples was estimated to have $H_0 \leq -14.5$, indicating the formation of superacidic sites. The correlation between catalytic activity and acidity holds for both reactions, cumene dealkylation and 2-propanol dehydration.

Acknowledgements. This work was supported by grant No. (R05-2003-000-10074-0) from the Basic Research Program of the Korea Science and Engineering Foundation. We wish to thank Korea Basic Science Institute (Daegu Branch) for the use of X-ray diffractometer.

References

1. Cheung, T. K.; d'Itri, J. L.; Lange, F. C.; Gates, B. C. *Catal. Lett.* **1995**, *31*, 153.
2. Tanabe, K.; Misono, M.; Ono, Y.; Hattori, H. *New Solid Acids and Bases*; Elsevier Science: Amsterdam, 1989; Chapter 4.
3. Olah, G. A.; Prakash, G. K. S.; Sommer, J. *Superacids*; Wiley-Interscience: New York, 1985; Chapter 2.
4. Arata, K. *Adv. Catal*. **1990**, *37*, 165.
5. Sohn, J. R. *J. Ind. Eng. Chem*. **2004**, *10*, 1.
6. Ward, D. A.; Ko, E. I. *J. Catal*. **1994**, *150*, 18.
7. Vaudagna, S. R.; Comelli, R. A.; Canavese, S. A.; Figoli, N. S. *J. Catal*. **1997**, *169*, 389.
8. Kustov, L. M.; Kazansky, V. B.; Figueras, F.; Tichit, D. *J. Catal*. **1994**, *150*, 143.
9. Sayari, A.; Yang, Y.; Song, X. *J. Catal*. **1997**, *167*, 346.
10. Hsu, C. Y.; Heimbuch, C. R.; Armes, C. T.; Gates, B. C. *J. Chem. Soc., Chem. Commun*. **1992**, 1645.
11. Cheung, T. K.; Gates, B. C. *J. Catal.* **1997**, *168*, 522.
12. Adeeva, V.; de Haan, H. W.; Janchen, J.; Lei, G. D.; Schunemann, V.; van de Ven, L. J. M.; Sachtler, W. M. H.; van Santen, R. A. *J. Catal*. **1995**, *151*, 364.
13. Wan, K. T.; Khouw, C. B.; Davis, M. E. *J. Catal*. **1996**, *158*, 311.
14. Song, X.; Reddy, K. R.; Sayari, A. *J. Catal*. **1996**, *161*, 206.
15. Coelho, M. A.; Resasco, D. E.; Sikabwe, E. C.; White, R. L. *Catal. Lett*. **1995**, *32*, 253.
16. Hosoi, T.; Shimadzu, T.; Ito, S.; Baba, S.; Takaoka, H.; Imai, T.; Yokoyama, N. *Prepr. Symp. Div. Petr. Chem*.; American Chemical Society: LosAngels, CA, 1988; p 562.
17. Ebitani, K.; Konishi, J.; Hattori, H. *J. Catal*. **1991**, *130*, 257.
18. Signoretto, M.; Pinna, F.; Strukul, G.; Chies, P.; Cerrato, G.; Ciero, S. D.; Morterra, C. *J. Catal*. **1997**, *167*, 522.
19. Hino, M.; Arata, K. *J. Chem. Soc., Chem. Commun*. **1987**, 1259.
20. Larsen, G.; Lotero, E.; Parra, R. D. *In Proceeding of the 11th International Congress on Catalysis*; Elsevier : New York, 1996; pp 543-551.
21. Arata, K.; Hino, M.; Yamagata, N. *Bull. Chem. Soc. Jpn*. **1990**, *63*, 244.
22. Sohn, J. R.; Kwon, T. D.; Kim, S. B. *J. Ind. Eng. Chem.* **2001**, *7*, 441.
23. Sohn, J. R.; Lee, J. S. *Bull. Korean Chem. Soc*. **2003**, *24*, 159.
24. Sohn, J. R.; Park, W. C.; Kim, H. W. *J. Catal*. **2002**, *209*, 69.
25. Sohn, J. R.; Bae, J. H. *Korean J. Chem. Eng*. **2000**, *17*, 86.
26. Sohn, J. R.; Park, M. Y. *Langmiur* **1998**, *14*, 6140.
27. Sohn, J. R.; Kim, H. W.; Park, M. Y.; Park, E. H.; Kim, J. T.; Park, S. E. *Appl. Catal. A: General* **1995**, *128*, 127.
28. Saur, O.; Benstitel, M.; Saad, A. B. H.; Lavalley, J. C.; Tripp, C. P.; Morrow, B. A. *J. Catal*. **1986**, *99*, 104.
29. Morrow, B. A.; McFarlane, R. A.; Lion, M.; Lavalley, J. C. *J. Catal*. **1987**, *107*, 232.
30. Yamaguchi, T. *Appl. Catal.* **1990**, *61*, 1.
31. Jin, T.; Yamaguchi, T.; Tananbe, K. *J. Phys. Chem.* **1986**, *90*, 4794.
32. Sohn, J. R.; Park, W. C. *Appl. Catal. A: General* **2003**, *239*, 269.
33. Hua, W.; Xia, Y.; Yue, Y.; Gao, Z. *J. Catal*. **2000**, *196*, 104.
34. Sohn, J. R.; Cho, S. G.; Pae, Y. I.; Hayashi, S. *J. Catal*. **1996**, *159*, 170.
35. Tanabe, K. *Solid Acids and Bases*; Kodansha, Tokyo, 1970; p 170.
36. Satsuma, A.; Hattori, A.; Mizutani, K.; Furuta, A.; MiyaMoto, A.; Hattori, T.; Murakami, Y. *J. Phys. Chem*. **1988**, *92*, 6052.
37. Sohn, J. R.; Park, E, H.; Kim, H. W. *J. Ind. Eng. Chem*. **1999**, *5*, 253.
38. Olah, F. G. A.; Prakash, G. K. S.; Sommer, J. *Science* **1979**, *206*, 13.

39. Miao, C.; Hua, W.; Chen, J.; Gao, Z. *Catal. Lett.* **1996**, *37*, 187.
40. Sohn, J. R.; Ryu, S. G. *Langmuir* **1993**, *9*, 126.
41. Sohn, J. R.; Lee, S. Y. *Appl. Catal. A: General* **1997**, *164*, 127.
42. Sohn, J. R.; Jang, H. *J. Mol. Catal.* **1991**, *64*, 349.
43. Decanio, S. J.; Sohn, J. R.; Paul, P. O.; Lunsford, J. H. *J. Catal.* **1986**, *101*, 132.
44. Sohn, J. R.; Chun, E. W.; Pae, Y. I. *Bull. Korean Chem. Soc.* **2003**, *24*, 1785.
45. Sohn, J. R.; Ozaki, A. *J. Catal.* **1980**, *61*, 29.
46. Sohn, J. R.; Park, W. C.; Kim, H. W. *J. Catal.* **2002**, *209*, 69.